A

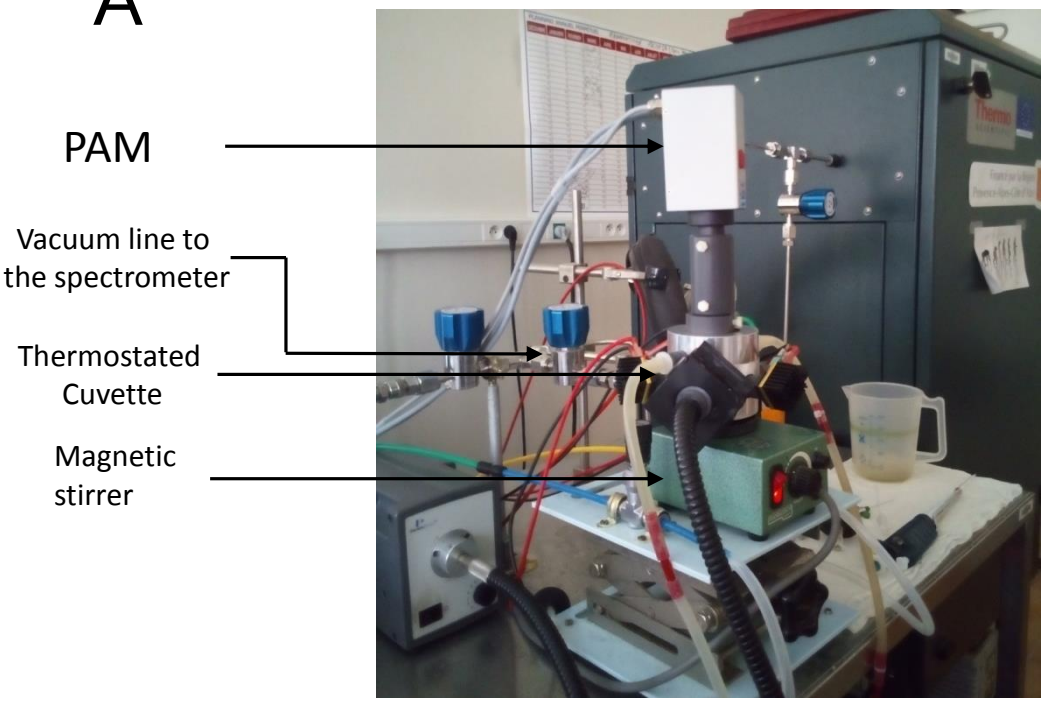

B

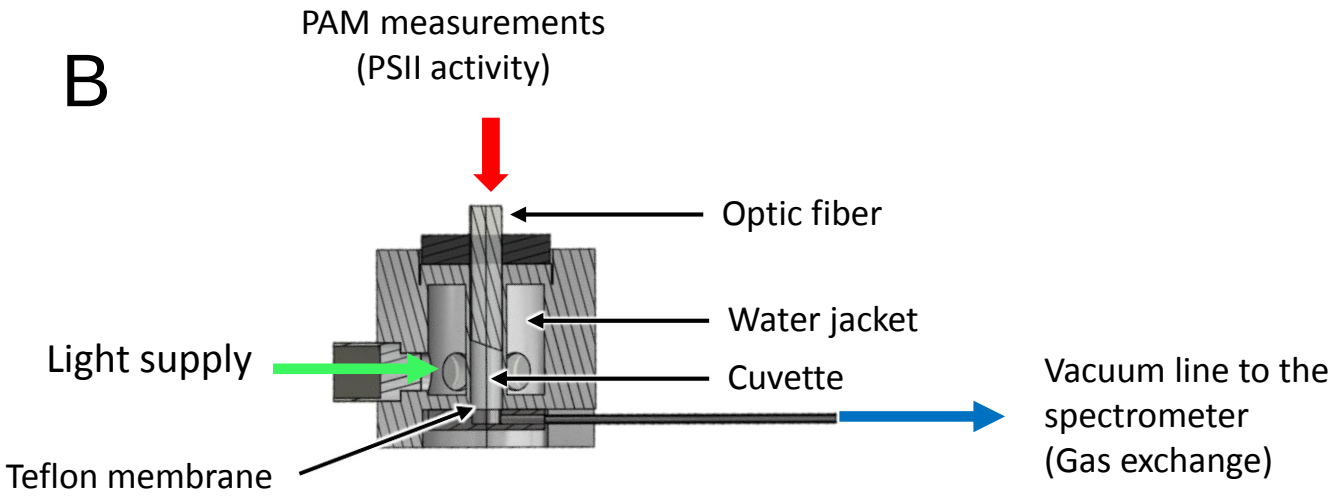

Supplemental Figure S1. Experimental device used for combined measurements of gas exchange by using MIMS and chlorophyll fluorescence with a PAM. A. Picture of the experimental device. B. Schematic view of the cuvette used for simultaneous measurements of fluorescence and mass spectrometry.

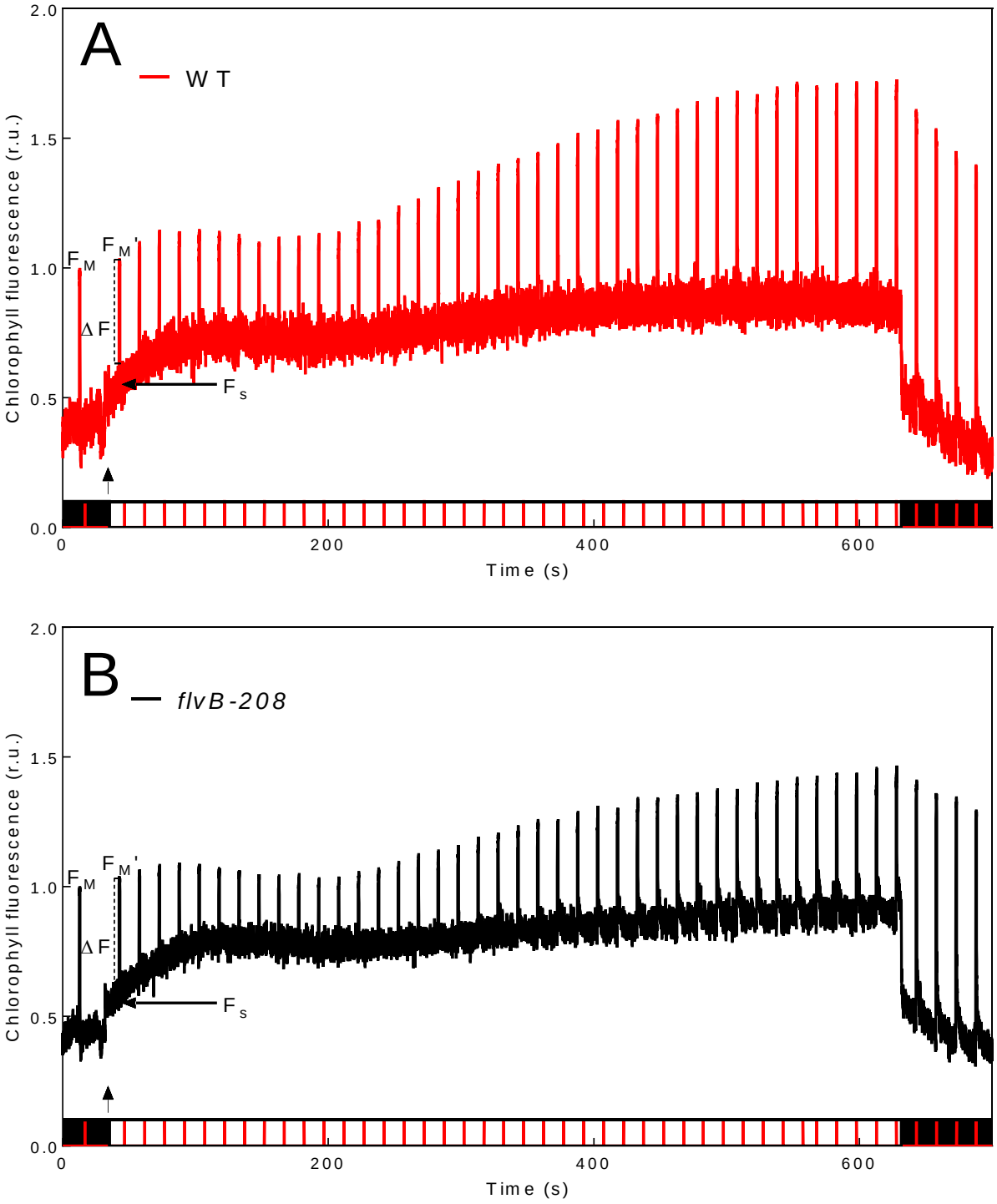

Supplemental Figure S2. Representative chlorophyll fluorescence recordings obtained during a dark to light transient in anaerobically acclimated *C. reinhardtii* cells. (A) wild-type strain (WT). (B) *flvB-208* mutant. Cells were harvested from photobioreactor cultures and placed in the MIMS cuvette. Chlorophyll fluorescence was recorded during a dark to light transient following 1h30 of dark anaerobic acclimation. Red spikes at the bottom of the figure show saturating flashes.

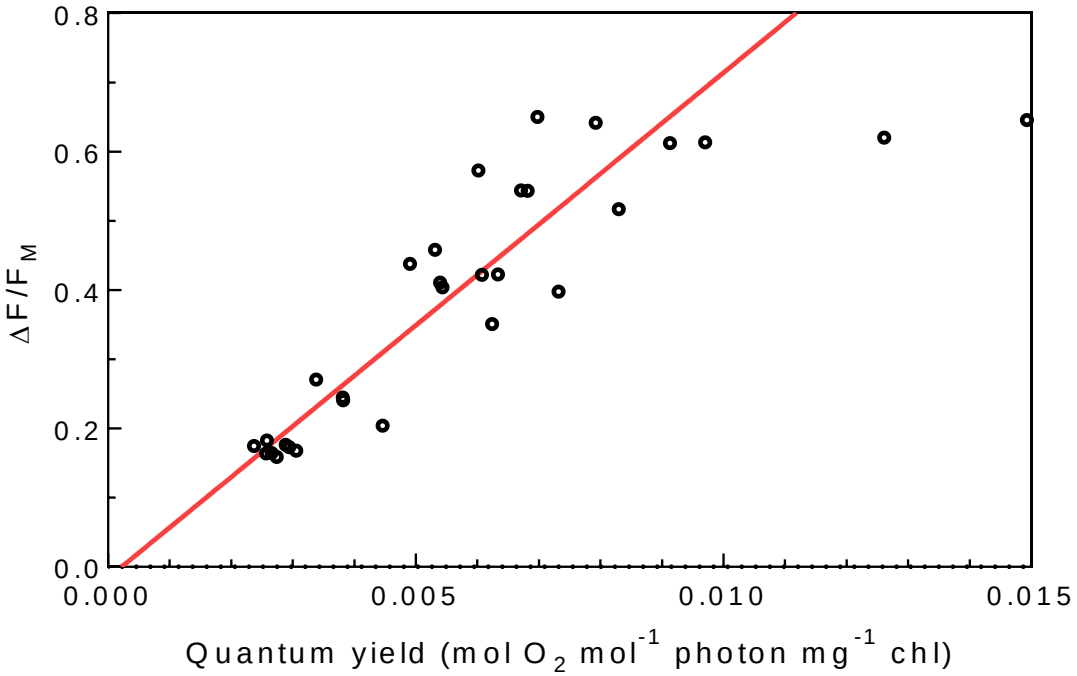

Supplemental Figure S3. Relationship between quantum yield of O_2 evolution and $\Delta F/F_M$ in aerobiosis at a low chlorophyll concentration. Chlorophyll fluorescence measurements were recorded using a PAM on top of a Hansatech cuvette linked to a Membrane Inlet Mass Spectrometer (MIMS). Recorded PSII yields were correlated with O_2 exchange measurements made with $^{18}O_2$ using the MIMS in aerobic conditions after 10 minutes dark adaptation. Experimental relation between the $\Delta F/F_M$ and the quantum yield of O_2 Evolution. In red is shown the linear regression for the points with a $\Delta F/F_M$ lower than 0.6. Chlorophyll concentration was set to 10µg Chl.mL^{-1}.

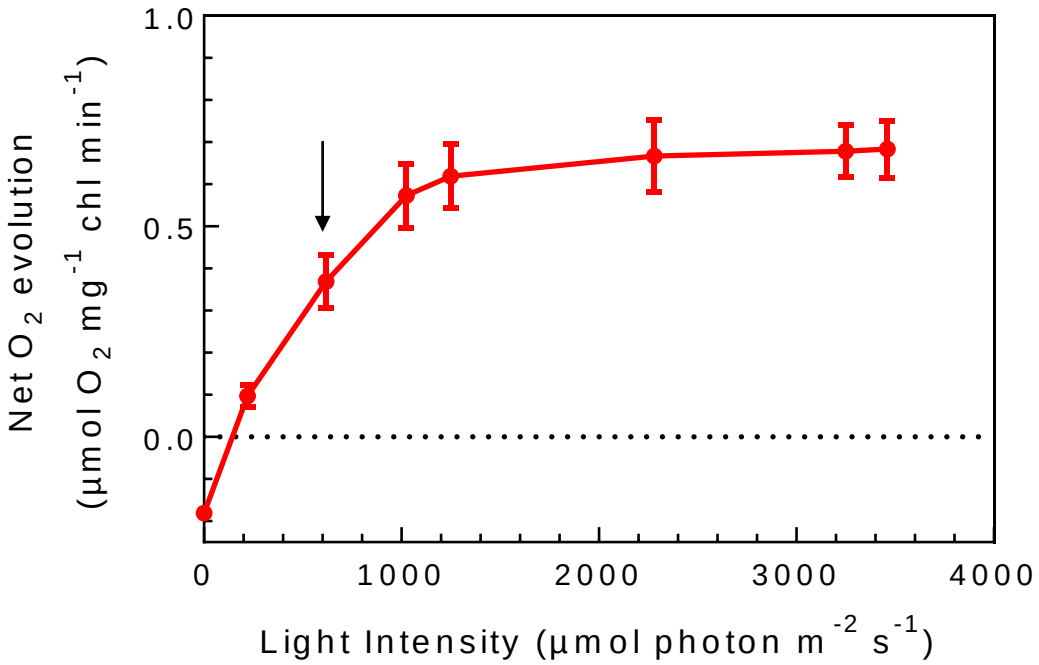

Supplemental Figure S4. Saturation curve of net photosynthesis with green light. Net O_2 evolution was measured with a MIMS after 1 min illumination at different green light intensities (mean +/- SD, n=5 biological replicates). The arrow indicates the light intensity used throughout this work.

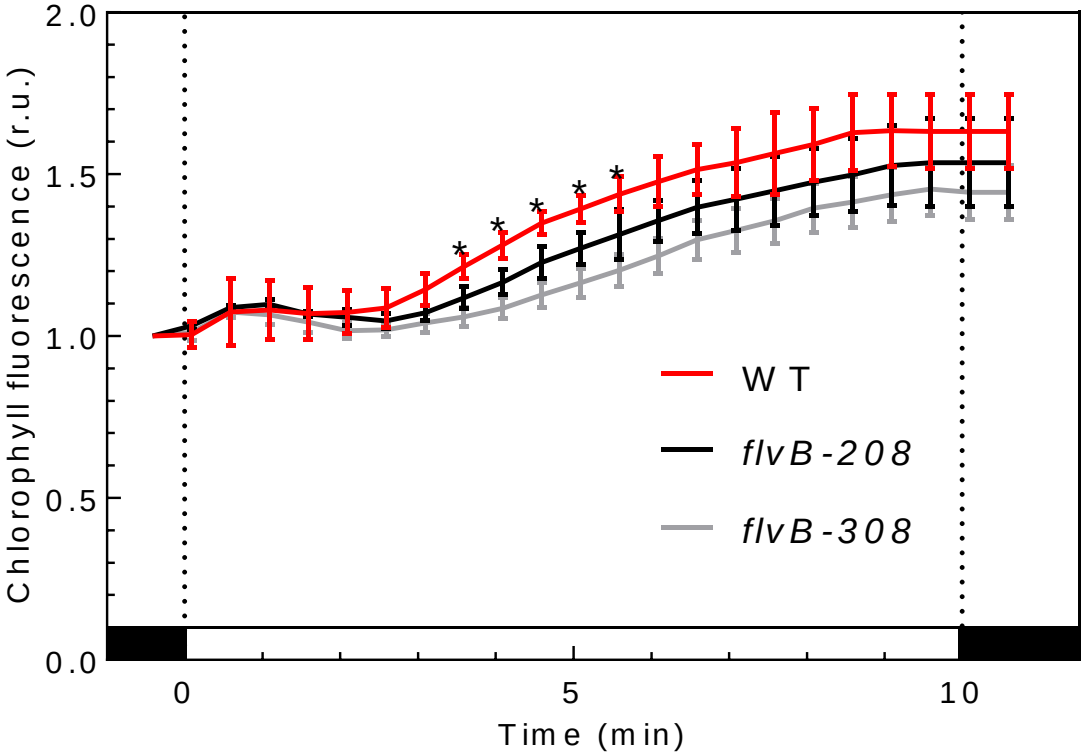

Supplemental Figure S5. Maximum fluorescence yield (F_M') upon a shift from dark anaerobiosis to light as a control for assessing PSII absorbance changes. Maximum fluorescence level during the first ten minutes of illumination. After 1h30 of dark anaerobic acclimation in the MIMS cuvette, algal suspensions of wild type (red line) and *flvB* mutant (grey and dark lines) strains were illuminated (660 µmol photons m^{-2} s^{-1} green light). Maximum chlorophyll fluorescence level was measured before illumination (F_M) and each 30s upon illumination (F_M'). Shown are mean values (+/-SD, n=3 for the mutants, n=6 for the WT), a star marks significant difference between the wt and the mutant strains (Pvalue <0.05) based on ANOVA analysis (Tukey adjusted P value). Fm' value at the onset of light was normalized to 1 (r.u. relative units).

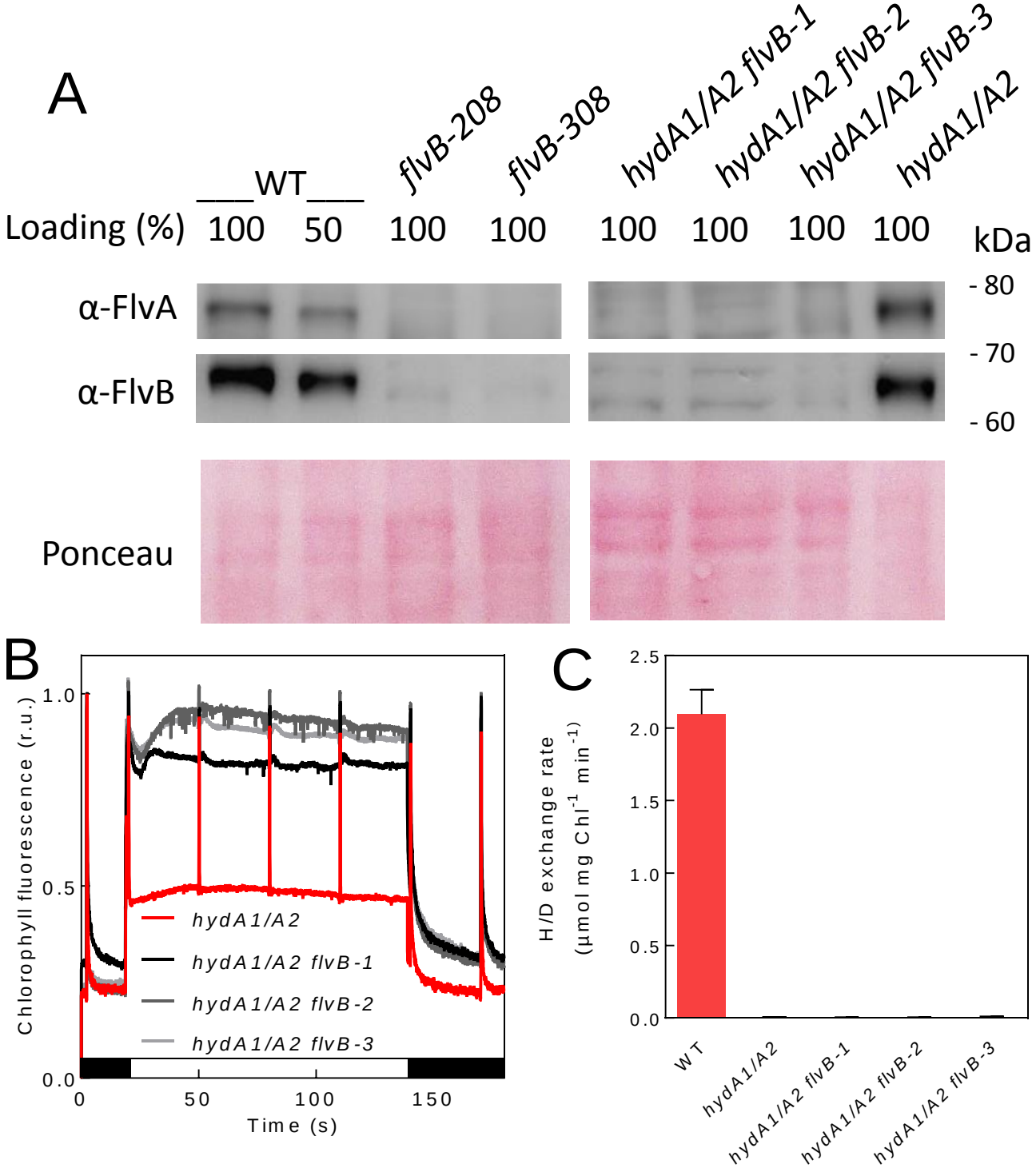

Supplemental S6. Characterization of the mutant *Chlamydomonas* cells. (A) Immunodetection of Flvs in anaerobically acclimated cells. *Chlamydomonas* cells were harvested from exponential phase, centrifuged, resuspended at the same concentration in HSM medium and hermetically sealed in glass flack. Cells were harvested after 3 hours anaerobiosis and immunodetection was done on total cell extract. (B) Aerobic chlorophyll fluorescence pattern of triple and double mutant. Cells were grown in TAP medium under low light and harvested during exponential phase. Chlorophyll fluorescence measurements were performed using pulse amplitude modulated fluorimeter in the dark (black boxes) and under red actinic light (100 µmol photon m^{-2} s^{-1}). Data are normalized on initial F_M measurements. (C) *In vivo* hydrogenase activities as measured by H/D exchange rates after 1h dark anaerobic acclimation. Shown are mean values (+/-SD, n=2 for the mutants, n=4 for the WT).

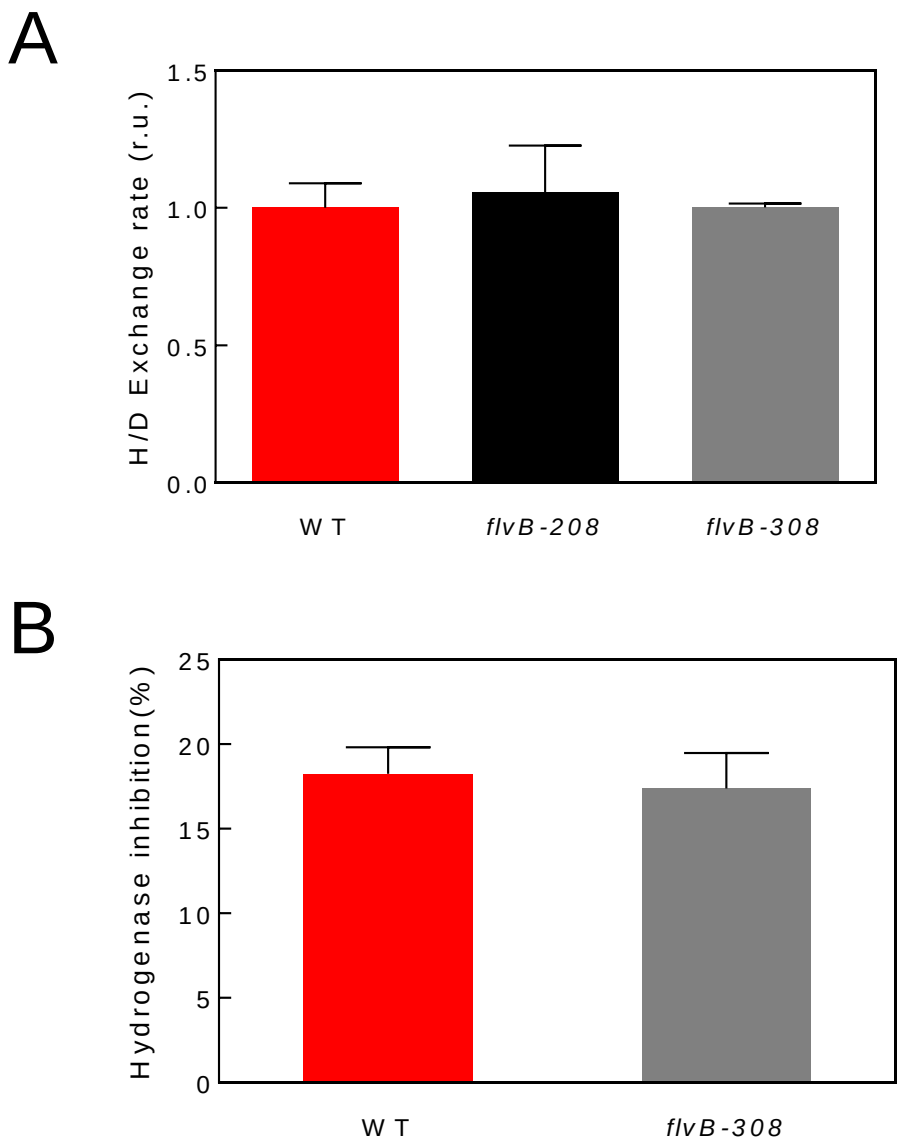

Supplemental Figure S7. Hydrogenase activity assayed *in vivo* by H/D exchange. After 1h30 of dark anaerobic acclimation in the MIMS cuvette, algal suspensions of wild type (red box) and *flvB* mutant (grey and dark box) strains were saturated with Deuterium (D_2). H_2, HD and D_2 were then recorded with a MIMS and H/D exchange rate was calculated (Jouanneau et al, 1980). (A) H/D exchange rates after dark anaerobic acclimation. Shown are mean values (+/-SD, n=2 for the mutants, n=4 for the WT). (B) Percentage of the inhibition of the H/D exchange rate after two minutes of illumination. Shown are mean values (+/-SD, n=2).

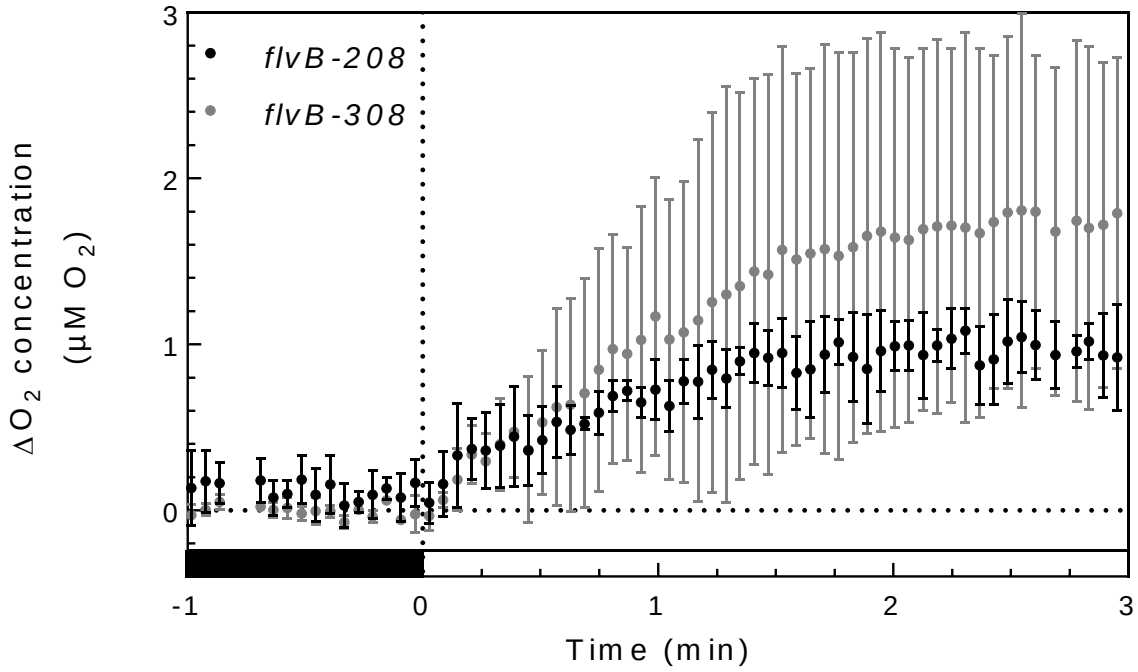

Supplemental Figure S8. Differences in O_2 concentration present in the MIMS chamber containing *flvB* mutants compared to the WT during a dark to light transient in anaerobically acclimated *C. reinhardtii*. Differences in O_2 concentration were calculated from absolute gas exchange as determined in Fig. 4. Shown are mean values of the following calculation for each of the two mutants : $[O_2]$(*flvB*)-$[O_2]$(WT) were $[O_2]$(flvB) and $[O_2]$(WT) are the O_2 level in a mutant or a WT cell suspension respectively (+/-SD, n=3).

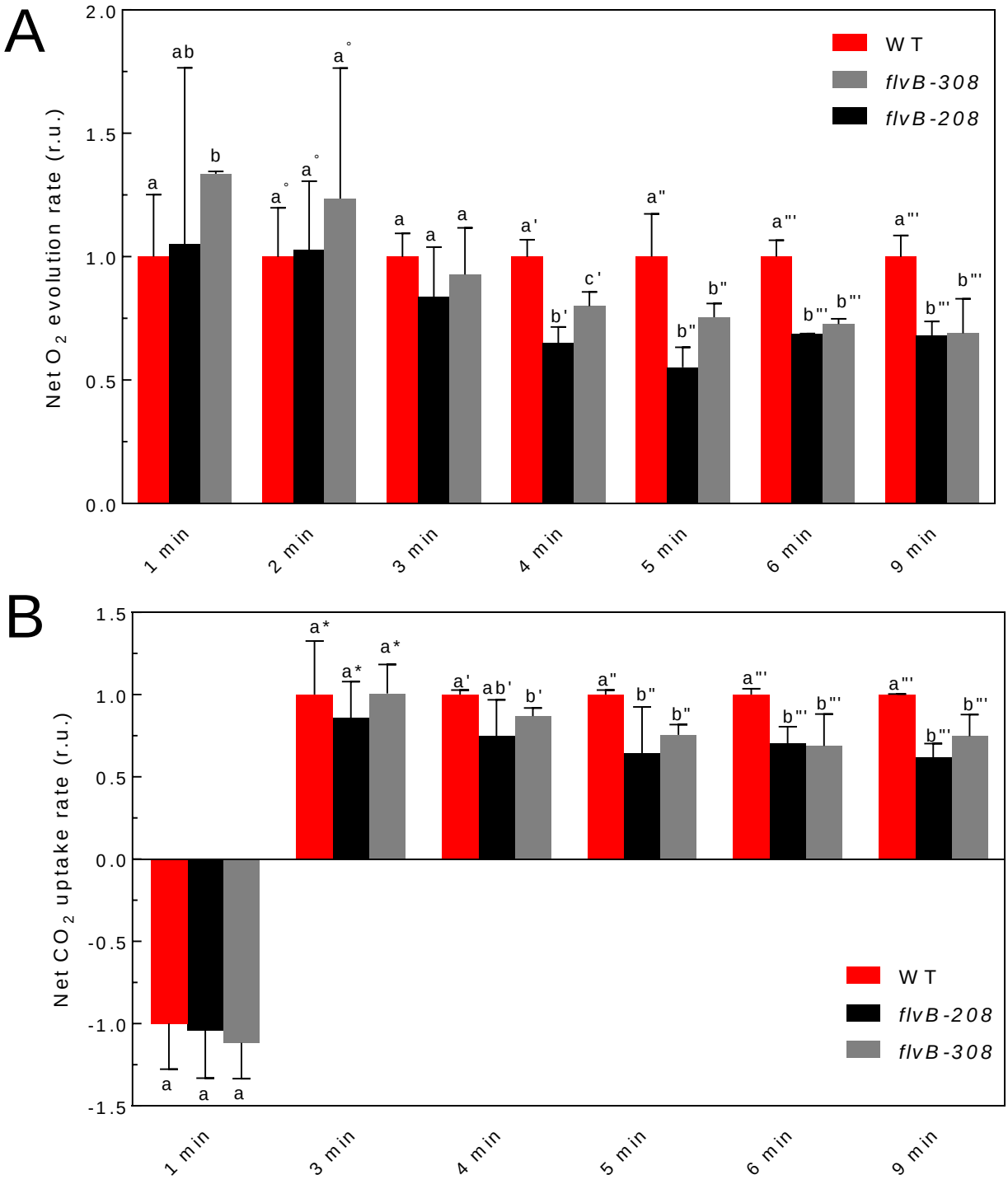

Supplemental Figure S9. Net O_2 and CO_2 exchange rates in the light in *C. reinhardtii* wild-type and two *flvB* mutants. After 95 min of dark anaerobic acclimation, WT (red) and two independent *flvB* mutant (*flvB-208* and *flvB-308*, dark and grey respectively) cell suspensions were illuminated (660 µmol photons m^{-2} s^{-1} green light). O_2 and CO_2 gas exchange were measured using a MIMS. (A). Mean values of net O_2 evolution (B) and net CO_2 uptake rates measured between 1 min and 9 min of illumination Shown are mean values relative to the absolute WT level at the same time point (+/-SD, n=3 for the mutants, n=6 for the WT).. Letters (a, b and c) above the bars represent statistically significant differences (P value=0.05) between strains for a given gas exchange measurement based on ANOVA analysis. Values for CO_2 at 2 min are all close to 0 and were not plotted for clarity of the other data.

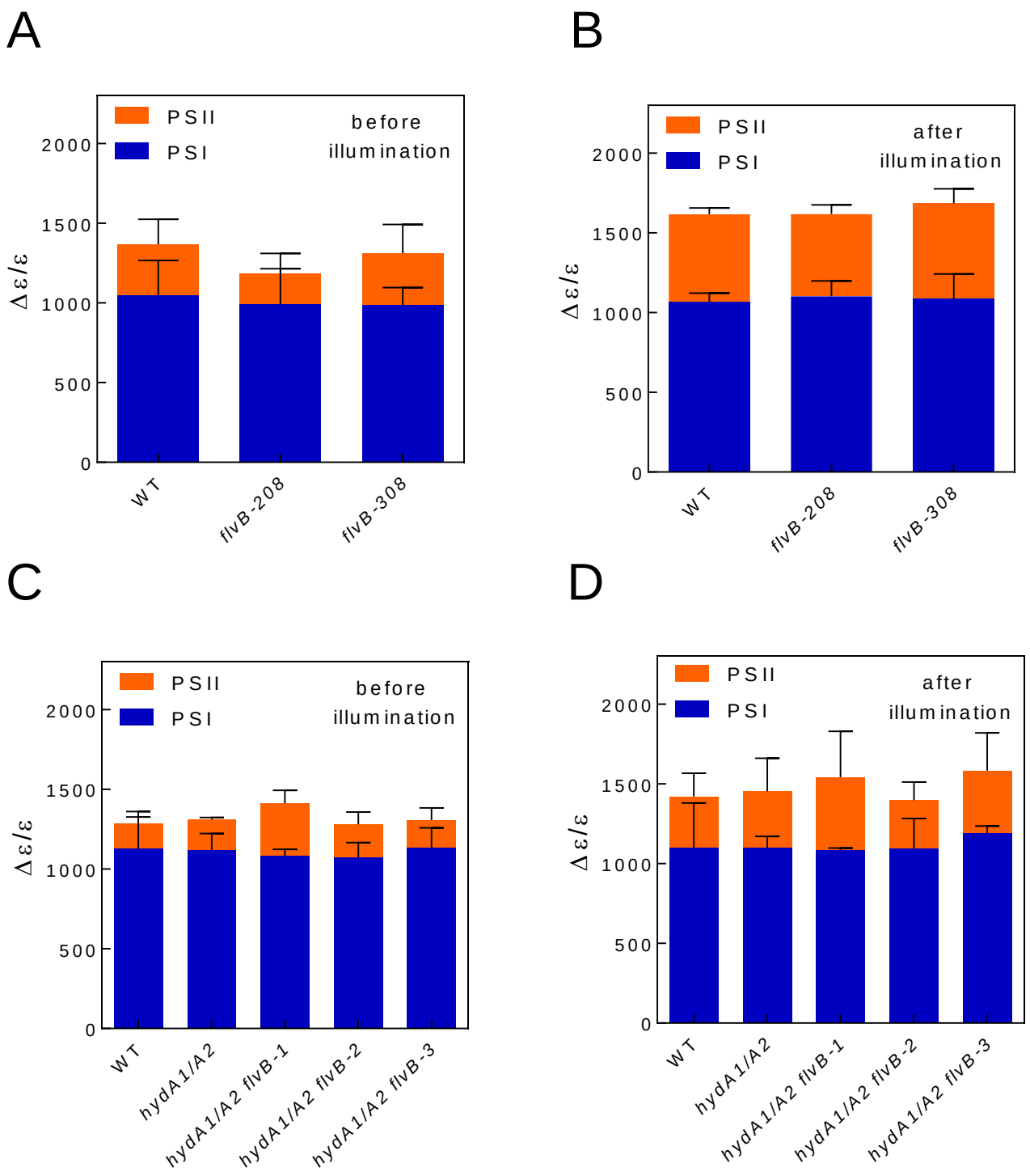

Supplemental Figure S10. PSI and PSII activities as measured by ElectroChromic Shift (ECS) upon illumination of anaerobically-acclimated *Chlamydomonas* cells. ECS at 520 nm was measured after 95 min anerobic acclimation of *Chlamydomonas* cells (A, C) and after a subsequent 10 min illumination (200 µmol photons m^{-2} s^{-1} white light) (B, D). (A, B) *flv* mutants are compared to the CC-4533 parental strain. (C, D) *hydA1/A2* mutants are compared to the CC-124 parental strain. Shown are means +/- SD (n=3, biological replicates).

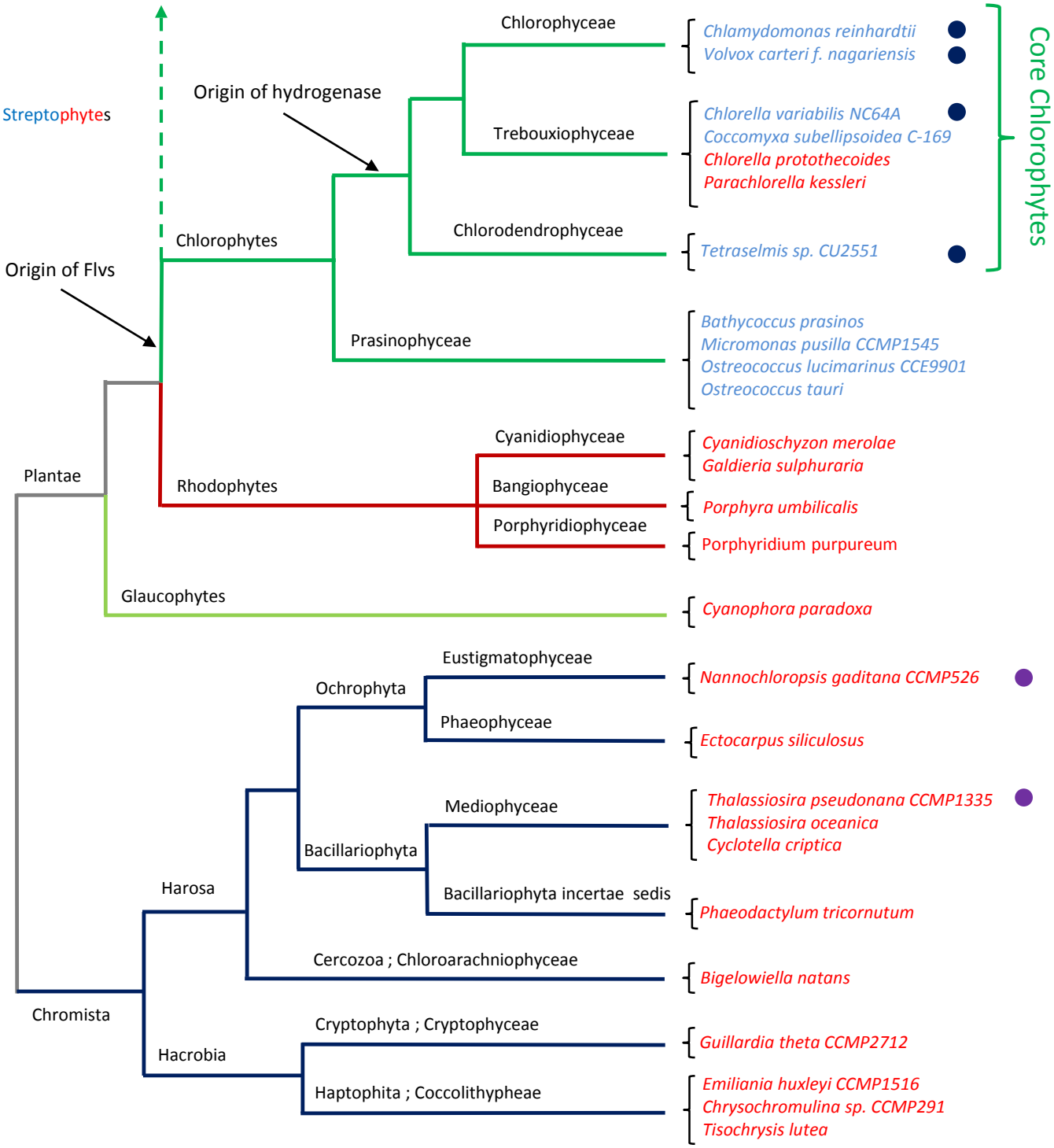

Supplemental S11. Repartition of Flavodiiron proteins (Flv) and [Fe-Fe] hydrogenase on the evolutionary tree of eukaryotic microalgae. The tree of life, representing the mains branchings between different classes of eukaryotic algae was drawn using previously published trees (Leliaert et al, 2012; Fucikova et al, 2014; Burlacot and Peltier, 2018) and sequenced organisms were placed on it. Absence of a Flavodiiron was defined as the absence of any gene meeting the requirements used in Supplemental Table 1. Presence or absence of Flvs is shown by the color of the organism name (respectively blue or red). Presence of a [Fe-Fe] hydrogenase in the genome is shown by a disc right of the organism name according to Burlacot and Peltier (2018), blue discs show the presence of hydrogenase with a known activity, purple circles show putative hydrogenases with a yet uncharacterized activity. In dashed line is shown the embranchment of streptophites with green algae (Martin and Melkonian, 2010). Proposed origin of genes are shown with arrows.

Organism	Class	Number of Flvs	Accession	Reference
Chlamydomonas reinhardtii	Chlorophyceae	2	XM_001699293.1 XM_001692864.1	Merchant et al, 2007
Volvox carteri f. nagariensis	Chlorophyceae	2	XM_002948441.1 XM_002948437.1	Prochnik et al, 2010
Chlorella variabilis NC64A	Trebouxiophyceae	2	XM_005849680.1 XM_005849412.1	Blanc et al, 2010
Coccomyxa subelisoida	Trebouxiophyceae	2	XM_005643392.1 XM_005643394.1	Blanc et al, 2012
Tetraselmis sp. GSL018	Chlorodendrophyceae	2	GBEZ01019221.1 GBEZ01009242.1	D'Adamo et al, 2014
Bathycoccus prasinos	Prasinophyceae	2	XM_007514037.1 XM_007514022.1	Moreau et al, 2012
Micromonas pusilla CCMP1545	Prasinophyceae	2	XM_003057449.1 XM_003056967.1	Worden et al, 2009
Ostreococcus lucimarinus CCE9901	Prasinophyceae	2	XM_001416063.1 XM_001416061.1	Palenik et al, 2007
Ostreococcus tauri	Prasinophyceae	2	XM_003075167.1 XM_003075163.1	Derelle et al, 2006

Supplemental Table S1. List of algae exhibiting a Flv in their genome. Genomic sequences of FlvA and FlvB from *Chlamydomonas reinhardtii* (https://phytozome.jgi.doe.gov/pz/portal.html Cre12.G531900 and Cre16.G691800 respectivelly) were BLAST against complete genome sequences of eukaryotic algae (https://blast.ncbi.nlm.nih.gov/Blast.cgi). Presence of a Flavodiiron protein was defined as the presence of a gene showing a similarity score higher than 200 for one of the two reference Flvs and coding for a protein having the 3 characteristic domains of eukaryotic Flvs (Romao et al, 2016).

Supplemental Material and methods:

Absorption change measurements. Carotenoid ElectroChromic Shift (ECS) was measured at 520 nm, using a JTS-10 (BioLogic, France). Cells were harvested from flasks cultures, centrifuged at 450g for 4 min and resuspended in a 3 mL glass cuvette in a buffer containing 20% Ficoll buffered with 20 mM HEPES (pH 7.2) at a final concentration of 20 µg Chl mL^{-1}. ECS signal was measured as the rapid increase of absorbance signal at 520 nm upon a saturating laser flash (6 ns, 680 nm, 1mJ). Respective contributions of PSI and PSII to the ECS signal were obtained accordingly to Bailleul et al (2010). Prior to measurement, cells were incubated for 90 min in anaerobiosis, some were eventually illuminated for 10 minutes.

Supplemental litterature cited :

Bailleul B, Cardol P, Breyton C, Finazzi G (2010) Electrochromism: a useful probe to study algal photosynthesis. Photosynth Res 106: 179-189

Blanc G, Agarkova I, Grimwood J, et al. (2012) The genome of the polar eukaryotic microalga Coccomyxa subellipsoidea reveals traits of cold adaptation. Genome Biology 13, R39.

Blanc G, Duncan G, Agarkova I, et al. (2010) The Chlorella variabilis NC64C genome reveals adaptation to photosymbiosis, coevolution with viruses, and cryptic sex. Plant Cell 22, 2943–2955.

Burlacot A, Peltier G (2018) Photosynthetic electron transfer pathways during hydrogen photoproduction in green algae: mechanisms and limitations. In M Seibert, G Torzillo, eds, Microalgal Hydrogen Production: Achievements and Perspectives. The Royal Society of Chemistry, pp 189-212

Derelle E, Ferraz C, Rombauts S et al. (2006) Genome analysis of the smallest free-living eukaryote Ostreococcus tauri unveils many unique features. Proceedings of the National Academy of Sciences, USA 103, 11647–11652.

D'Adamo S, Jinkerson RE, Boyd ES, Brown SL, Baxter BK, et al. (2014) Evolutionary and Biotechnological Implications of Robust Hydrogenase Activity in
Halophilic Strains of Tetraselmis. PLoS ONE 9(1): e85812. doi:10.1371/journal.pone.0085812

Fučíková, K., Leliaert, F., Cooper, E. D., Škaloud, P., D'Hondt, S., De Clerck, O., et al. (2014). New phylogenetic hypotheses for the core Chlorophyta based on chloroplast sequence data. Front. Ecol. Evol. 2: 63. doi: 10.3389/fevo.2014.00063

Leliaert F, Smith DR, Moreau H, Herron MD, Verbruggen H, Delwiche CF, De Clerck O (2012) Phylogeny and molecular evolution of the green algae. Crit Rev Plant Sci 31: 1–46

Marin, B., and Melkonian, M. (2010). Molecular phylogeny and classification of the Mamiellophyceae class. nov. (Chlorophyta) based on sequence comparisons of the nuclear- and plastid-encoded rRNA operons. Protist 161, 304–336. doi: 10.1016/j.protis.2009.10.002

Merchant SS, Prochnik SE, Vallon O, et al. (2007) The Chlamydomonas genome reveals the evolution of key animal and plant functions. Science 318, 245–251.

Moreau H, Verhelst B, Couloux A, et al. (2012) Gene functionalities and genome structure in Bathycoccus prasinos reflect cellular specialization at the base of the green lineage. Genome Biology 13, R74

Palenik B, Grimwood J, Aerts A et al. (2007) The tiny eukaryote Ostreococcus provides genomic insights into the paradox of plankton speciation. Proceedings of the National Academy of Sciences, USA 104, 7705–7710.

Prochnik, S.E., Umen, J., Nedelcu, .M. et al. (2010) Genomic analysis of organismal complexity in the multicellular green alga Volvox carteri. Science, 329, 223–226.

Worden AZ, Lee JH, Mock T et al. (2009) Green evolution and dynamic adaptations revealed by genomes of the marine picoeukaryotes Micromonas. Science 324, 268–272.

Romão C, Vicente J, Borges P, Frazão C, Teixeira M (2016) The dual function of flavodiiron proteins: oxygen and/or nitricoxide reductases. J. Biol. Inorg. Chem., DOI 10.1007/s00775-015-1329-4